Valuation of Energy Storage Operation in an AC Power Flow Model

Zora Luburić and Hrvoje Pandžić
Faculty of Electrical Engineering and Computing, University of Zagreb
Zagreb, Croatia
zora.luburic@fer.hr;
hrvoje.pandzic@fer.hr

Miguel Carrión
School of Industrial Engineering of Toledo, University of Castilla-La Mancha, Toledo, Spain
miguel.carrion@uclm.es

Tomislav Plavšić
Croatian TSO
HOPS
Zagreb, Croatia
tomislav.plavsic@hops.hr

***Abstract*—High integration of renewable sources in power systems requires additional assets that can sustain reduced controllability and increased variability of these sources. Energy storage has emerged as a flexible asset that increases flexibility and ensures a more economic and secure power system operation. This paper integrates large-scale battery energy storage in power system under different levels of wind power penetration. As opposed to many models already available, we use the full AC model approach that accurately represents power system operation, but at a cost of high computational burden. The proposed model is applied to the IEEE 24-bus test case modeled in GAMS environment and solved with. The power system operation is simulated with and without battery energy storage to show its contribution to the reduction of power system operating costs.**

Keywords: unit commitment, active and reactive optimal power flow, energy storage

I. Introduction

Unit commitment is a short-term decision-making problem, usually solved for the 24-hour time horizon [1]. It determines the generator commitment decisions and estimates their production levels at each hour while meeting the generator, system, network, and environmental constraints [2]. With the integration of renewable power sources into power systems, the operation of battery energy storage (BES) units is becoming more and more common [3]. Although there are different BES ownership models (see [4]), effects of BES on power system operation is best understood in typical unit commitment models, e.g. [5] and [6].

In this paper, we also assume a typical unit commitment problem, where the system operator is in charge of delivering electricity to its customers, as well as setting the operating points of generators and BES in the most cost-effective way. The objective function is the minimization of total system operating costs. Power system operation is represented using a rectangular representation of optimal power flow constraints, which is related to the full AC model [7].

Most research papers accommodate models that use the DC representation of power flows, which considers only active power flows and disregard network losses, to obtain convex solutions and shorter computation times. For instance, the authors in [5] propose a method for siting and sizing of energy storage in the highly renewable power system. The proposed approach consists of a three-stage planning procedure, where the optimal operation of new storage units is determined to alleviate congestion in the network and, consequently, reduce power system operating costs. It is concluded that the location and capacity of storage units is dependent on the distribution of wind resources and their level of penetration. Another use of DC power flow is demonstrated in [9], where a significant reduction of wind curtailment is obtained by introducing energy storage system in both the unit commitment and market clearing environment. Deterministic unit commitment model proposed in [10], also uses the DC representation of power flows and co-optimizes controllable conventional generators and energy storage units. The decrease in operating costs is obtained without distortion of the system reliability.

In general, if a renewable-dominant environment is considered, many models use a stochastic unit commitment model. The impact of significant uncertainties in both wind production and load are researched in [11]. Authors show that, by comparing the operating costs with the planned operation and the performance of the provided schedules, the stochastic optimization results in lower system operating costs. Also, they conclude that with a high value of wind production, the need for reserve is decreased. An important conclusion is that the peaking units' operation and power flows on interconnections are significantly modified. A parallel implementation of the Lagrangian relaxation is presented in [12] to solve the stochastic unit commitment under a set of scenarios using two different approaches: i) narrowing the duality gap of the Lagrangian, and ii) increasing the number of scenarios in order to obtain a more efficient power system operation schedule. It is shown that the first tested approach yields comparable benefits to the one with an increased scenario set, in the case of a reliable scenario selection algorithm.

As opposed to [4]-[12], which use DC power flow representation, AC network models that consider both the active and reactive power flows are used in [13]-[18]. Full AC models cannot be easily applied to large networks. The

This work has been supported in part by Croatian Science Foundation and Croatian Transmission System Operator (HOPS) under the project Smart Integration of RENewables (I-2583-2015) and with the project DPI2015-71280-R MINECO/FEDER, UE.

authors in [15] examine the DC and the AC model with Benders decomposition. They conclude that switching from the DC representation to the AC should be accompanied with additional auxiliary constraints. The importance of balancing economic and security issues in restructured markets is discussed in [16]. The proposed model is a security-constrained unit commitment model with additional system constraints: time-limited emergency controls for a given contingency and fuel and emission limits. Moreover, to solve a non-convex mixed-integer nonlinear program, authors in [17] propose a solution technique that co-optimizes both active and reactive power scheduling and dispatch under the AC optimal power flow and unit commitment constraints. The proposed model can be extended to use security constraints.

II. Methodology

The following assumptions are considered: i) we assume an economic dispatch problem, where binary variables modeling the generator commitments are neglected; ii) as common in the literature, energy scheduling of energy storage and wind power units is made considering that they only provide active power. The proposed model is tested with and without energy storage units and its formulation includes active and reactive power flow constraints using real complex equations.

Unlike the DC formulation, the full AC formulation includes the voltage magnitudes, reactive power flows, and network losses. The proposed model uses a rectangular representation of the optimal power flow constraints and is based on model from [14]. For convenience, the notation used in this formulation is listed in appendix at the end of the paper.

$$\underset{\aleph_t}{\text{Minimize}} \sum_t \sum_i Pg_{t,i} \cdot o_i \cdot \text{Z} \tag{1}$$

subject to:

$$\sum_{w \in M^n} Pw_{t,w} + \sum_{i \in M^n} Pg_{t,i} - \sum_{o(l) \in M^n} P_{t,l} + \sum_{d(l) \in M^n} P_{t,l} = PD_{t,n} \forall n \in \Omega^N,\ \forall t \in \Omega^T \tag{2}$$

$$\sum_{i \in M^n} Qg_{t,i} - \sum_{o(l) \in M^n} Q_{t,l} + \sum_{d(l) \in M^n} Q_{t,l} = QD_{t,n} \quad \forall n \in \Omega^N,\ \forall t \in \Omega^T \tag{3}$$

$$0 \le Pg_{t,i} \le Pg_i^{\max} \quad \forall i \in \Omega^I,\ \forall t \in \Omega^T \tag{4}$$

$$Qg_{t,i}^{\min} - \kappa_{t,i}^{Q\min} \le Qg_{t,i} \le Qg_{t,i}^{\max} + \kappa_{t,i}^{Q\max} \quad \forall i \in \Omega^I,\ \forall t \in \Omega^T \tag{5}$$

$$P_{t,l} = Y_l \left[V_{t,n}^2 \cdot \cos(\vartheta_l) - V_{t,n} \cdot V_{t,m} \cdot \cos(\theta_{t,n} - \theta_{t,m} - \vartheta_l)\right] \quad \forall \{n,m\} \in l \in \Omega^L,\ \forall t \in \Omega^T \tag{6}$$

$$Q_{t,l} = -Y_l \left[V_{t,n}^2 \cdot \sin(\vartheta_l) + V_{t,n} \cdot V_{t,m} \cdot \sin(\theta_{t,n} - \theta_{t,m} - \vartheta_l)\right] \quad \forall \{n,m\} \in l \in \Omega^L,\ \forall t \in \Omega^T \tag{7}$$

$$P_{t,l}^2 + Q_{t,l}^2 \le (S_l^{\max})^2 \quad l \in \Omega^L,\ \forall t \in \Omega^T \tag{8}$$

$$V_n^{\min} - \kappa_{t,n}^{V\min} \le V_{t,n} \le V_n^{\max} + \kappa_{t,n}^{V\max} \quad \forall n \in \Omega^N,\ \forall t \in \Omega^T \tag{9}$$

$$Pg_{t,i} - Pg_{t-1,i} \le RU_i \quad \forall i \in \Omega^I,\ \forall t \in \Omega^T \tag{10}$$

$$Pg_{t,i} - Pg_{t-1} \ge -RD_i \ \forall i \in \Omega^I,\ \forall t \in \Omega^T \tag{11}$$

$$soc_{t,s} = soc_{t,s}^{\text{in}} + p_{t,s}^{\text{ch}} \cdot \eta_s^{\text{ch}} - \frac{p_{t,s}^{\text{dis}}}{\eta_s^{\text{dis}}} \quad \forall s \in \Omega^S, t \in 1 \tag{12}$$

$$soc_{t,s} = soc_{t-1,s} + p_{t,s}^{\text{ch}} \cdot \eta_s^{\text{ch}} - \frac{p_{t,s}^{\text{dis}}}{\eta_s^{\text{dis}}} \quad \forall s \in \Omega^S, t \in \Omega^T \setminus \{1, T\} \tag{13}$$

$$soc_{t,s} \ge soc_{t,s}^{\text{in}} \quad \forall s \in \Omega^S, t \in T \tag{14}$$

$$soc_s^{\min} \le soc_{t,s} \le soc_s^{\max} \quad \forall s \in \Omega^S, t \in \Omega^T \tag{15}$$

$$p_{t,s}^{\text{ch}} \le ch_s^{\max} \cdot x_{t,s}^{\text{ch}} \quad \forall s \in \Omega^S, t \in \Omega^T \tag{16}$$

$$p_{t,s}^{\text{dis}} \le dis_s^{\max} \cdot (1 - x_{t,s}^{\text{ch}}) \quad \forall s \in \Omega^S, t \in \Omega^T \tag{17}$$

$$-\theta^{\max} \le \theta_{t,n} \le \theta^{\max} \quad \forall n \in \Omega^N,\ \forall t \in \Omega^T \tag{18}$$

$$Pw_{t,w} + ws_{t,w} = Pw_{t,w}^{\text{det}} \quad \forall w \in \Omega^W,\ \forall t \in \Omega^T \tag{19}$$

Optimization variables of full AC model are the elements of set:

$$\aleph_t = \left\{ g_{t,i},\ P_{t,l},\ Qg_{t,i},\ Q_{t,l},\ \kappa_{t,i}^{Q\min},\ \kappa_{t,i}^{Q\max},\ V_{t,n},\ \theta_{t,n},\ Pw_{t,w},\ ws_{t,w},\ soc_{t,s}, p_{t,s}^{\text{ch}},\ p_{t,s}^{\text{dis}},\ x_{t,s}^{\text{ch}} \right\}.$$

Objective function (1) minimizes total generation costs. Equations (2)-(3) present active and reactive power balance at each bus n. Inequality (4) limits the generators' production between their maximum and minimum power outputs (assumed to be zero), while inequality (5) imposes minimum and maximum limits of their reactive power outputs. Active power flows are determined by equation (6), and reactive power flows by (7). Their relationship is established by inequality (8), which defines a circular P-Q plane of the possible solutions. Voltage magnitudes are limited by their lower and upper bounds in (9). Ramp up and down limits are imposed by (10)-(11). Battery energy storage constraints are (12)-(17).

Battery state of charge depends on the initial battery state of charge, as formulated in (12). The first item considers the initial state of charge, and depending on the charging or discharging period, the battery is charged by the second item, or discharged by the third item. Equation (13) calculates the state of charge for the remaining time periods. The state of charge in the last hour should not be lower than the initial one, which is set by (14). Minimum and maximum limits on storage state of charge are imposed by constraint (15). Power charging and discharging limits are enforced by (16) and (17). Upper and lower limits on voltage angles are imposed by (18). Used wind power and wind power spillage are equal to the available wind power production in (19).

III. Case Study

The proposed models are tested on a case study based on the IEEE 24-bus system test case [18]. The original system has been modified including 7 wind farms in the upper part of the power system, and two battery energy storage units at buses 15 and 19, as shown in Figure 1. Data for this case study are taken from [19]. All simulations are performed under GAMS 24.9.1 on a Linux-based server with 11 2.9-GHz processors and 250 GB of RAM. CONOPT solver is used for solving the full AC formulation without BES units and DICOPT for solving the full AC formulation with BES units. Load data (active and reactive power) used in this model are represented in the upper graph in Figure 2. Peak active load is 2,513 MW and it appears during the late afternoon in hours 18-19. Overall daily active energy consumption is 50 GWh, and reactive is 5 GVArh.

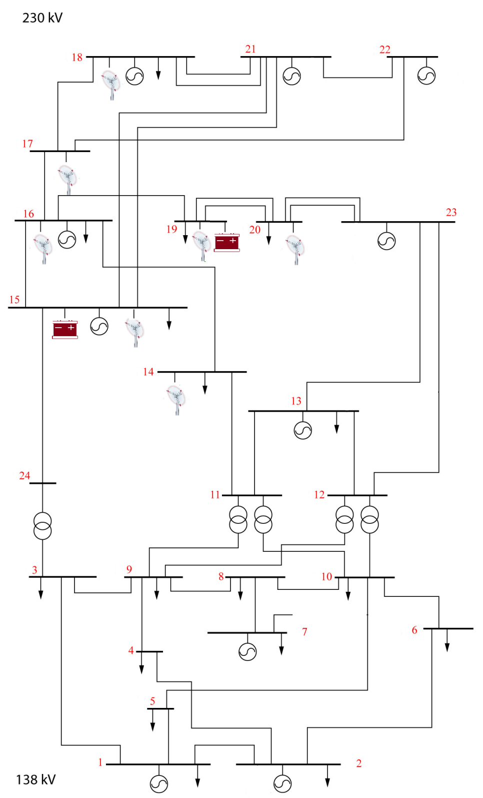

Fig. 1. IEEE 24-bus system test case

The lower graph in Figure 2 shows the wind production available in the considered day by each wind farm. This case is considered as wind factor $f = 1.0$. Total wind production is 49 GWh and is denoted as $Pw_{t,w}^{\text{det,ini}}$. Wind speed data are available in [19]. Wind production is very high throughout the day, but varies across location. For example, wind farm w4 produces at its maximum until hour 14, and then in the second part of day its production drops almost to 30% of its installed capacity. Wind farm w6 produces almost 100% the first two hours and during hours 4-10 does not produce at all. After hour 10, the available wind output is around 50% of the installed capacity and at hours 23-24 it reaches the maximum production level. These two wind farm output examples show how much variability wind power can introduce in a power system.

In case when there is more available wind power than needed in the power system, a part of the wind power production is curtailed. In these cases the battery storage systems take their major role, as they store excess electricity and inject it back into the network when needed. This article analyzes how different wind factor levels (lower and higher than the power outputs in the lower graph of Figure 2) affect the total generation costs. Each BES unit has maximum state of charge 120 MWh and maximum charging/discharging power 40 MW. It is assumed that the energy efficiencies of both charging and discharging processes are 0.9.

TABLE I
TOTAL OPERATING COSTS (TOC) IN THE FULL AC MODEL WITH/WITHOUT BES UNDER DIFFERENT LEVELS OF WIND PENETRATION

Model	Wind factor f	TOC without BES (€)	TOC with BES (€)	TOC savings with BES (%)
Full AC	0	713,741	713,294	0.06
	0.5	275,003	273,230	0.65
	1	48,135	46,049	4.33
	1.5	13,869	11,218	19.11

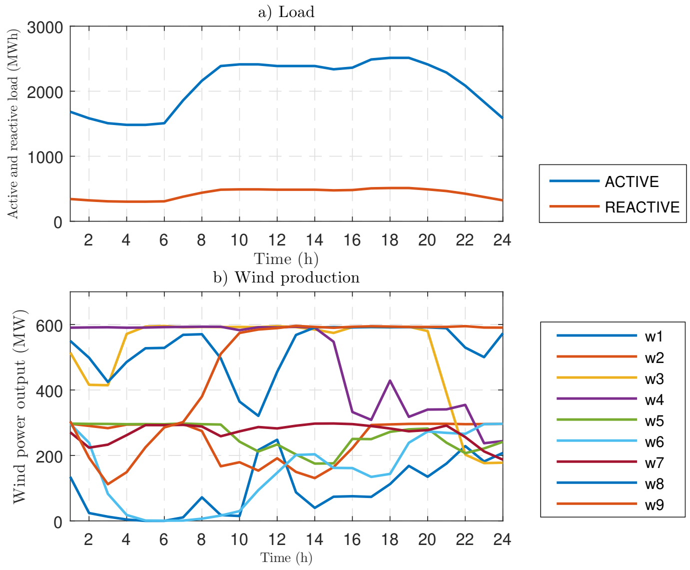

Fig. 2. Active and reactive load (upper graph), and wind production of 7 wind farms under the initial wind factor (lower graph).

IV. RESULTS

Table I shows the total operating costs (TOC) under different wind penetration levels pertaining to factor f. In this manner, the available wind power production is computed as $Pw_{t,w}^{\text{det}} = f \cdot Pw_{t,w}^{\text{det,ini}}$. With no wind in the system, TOC obtained using the full AC power flow formulation are the highest and amount to €713,741. Observe that the differences between TOC obtained in proposed model decreases as the wind power penetration increases. It should be noted that introducing BES decreases TOC in all cases. In case when there is no wind in the system, TOC are only slightly decreased, by 0.06%. For wind penetration factor f of 0.5, TOC are reduced by 0.65%. TOC savings for wind penetration factor 1 are significantly higher, 4.33%. When increasing wind factor to 1.5, the proposed model has very low TOC, only €13,869 without BES with additional 19.11% savings with BES operation.

Figure 3 shows the overall wind curtailment for different wind power penetration factors. For factor 0.5, there is no wind spillage. However, for wind energy penetration factor 1.0 wind curtailment increases raises to 3,375 MWh without the BES devices and 3,155 MWh with BES in operation. The highest wind curtailment (23,221 MWh) is achieved for 1.5

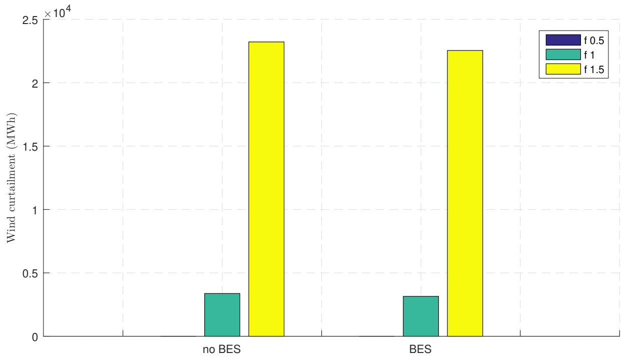

Fig. 3. Wind curtailment for different wind penetration factors

wind penetration factor when there is no BES. Introduction of BES devices reduces slightly wind spillage by 2.89%.

Active power losses are shown in Table II. With increased wind generation, active power losses in the full AC model increase as well. The most noticeable difference in active power losses under different factor is the one between the state where there is no wind and under wind power factor of 0.5, where the active power losses are increased by 692 MWh. Introducing BES in the power system with no wind power results in 2 MWh reduced active power losses. For all the other wind factors, the active power losses are slightly increased after the introduction of BES.

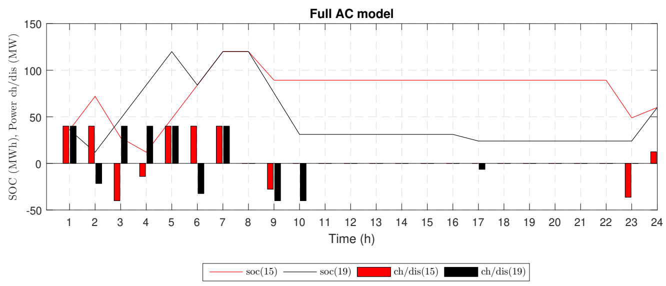

Fig. 4. BES state of charge and charging and discharging quantities at buses 15 and 19 in the full AC model for wind penetration level equal to 1

Figure 4 represents the BES operation for wind penetration level equal to 1. BES units are more active in the first part of the day. The main reason is high level of wind power and low demand during the night and, consequently, absence of thermal generation until hour 8, as can be seen in Figure 5. Low BES activity in the second part of the day is closely related to the available wind generation shown in the lower graph in Figure 2. Both BES units are charged in hour 1 and then discharged in hour 2. BES at bus 15 is charged in hours 3-4 and then discharged in hour 5 due to low wind production of wind farm w2 at the same bus. However, it is charged up to its capacity in hour 7. The other BES unit (bus 19) is charged in hour 3, discharged in hour 4, and then charged up to its capacity in hour 7 as well. Both BES units discharge during the morning peak hours 9-10, and the BES at bus 19 performs a small discharge in the afternoon, while the BES unit at bus 15 discharges in hour 23. Finally, this BES charges in the last hour to reach the required 50% state of charge at the end of the day.

To better understand the resulting total operation costs of the proposed model with BES operation and for wind penetration level equal to 1, generator committed statuses are shown in Figure 5. The most used generators are 22 and 23 at buses 18 and 21, respectively. These generators are nuclear and operate at the lowest cost. All generating units are started at hour 8. Referring to these results, it can be seen that high level of renewable power in the system results in few generating units in operation. The full AC model without BES has higher generation cost due to committed unit 12 in hours 9-10 with cost of 17.19 €/MWh, and unit 9 in hour 23 with cost of 17.59 €/MWh. BES unit replaces these generators units and decreases overall system operating costs.

Figure 6 shows voltage magnitudes at buses 15 and 19 and the differences in voltage levels with and without the BES in operation. The different voltage levels appear only during BES operation - compare to Figure 4. During the charging process of the BES unit in hours 1 and 2, voltage magnitude at bus 15 is slightly decreased, and while the BES is discharged in hours 3-4, voltage magnitude is higher. Again, the voltage is decreased due to charging of the BES in hours 5-7. In hours 9-10, the voltage magnitudes are closer to their nominal value (1 p.u.). There are no voltage magnitude differences in the second part of the day due to the BES inactivity in this period. Similar results are obtained for bus 19, where the other BES is installed. In general, voltage magnitudes at buses 15 and 19 are very close to their nominal value (1 p.u.).

Execution times of the proposed model are listed in Table III. Generally, the formulation that includes BES operation

TABLE II

TOTAL ACTIVE POWER LOSSES IN THE FULL AC MODEL WITH AND WITHOUT BES FOR DIFFERENT LEVELS OF WIND PENETRATION

Model	Wind factor f	Active power losses without BES (MWh)	Active power losses with BES (MWh)
Full AC	0	338	336
	0.5	1,030	1,041
	1	1,766	1,774
	1.5	1,804	1,809

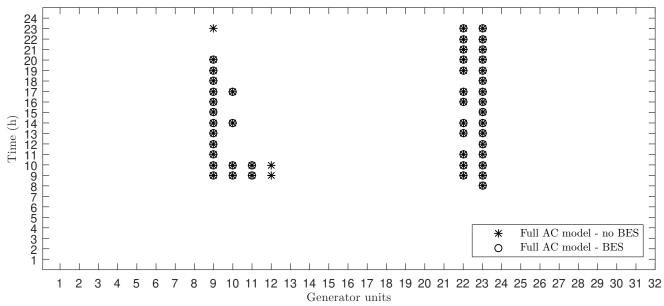

Fig. 5. Generator on/off statuses for the full AC model with and without BES in operation for wind penetration level equal to 1

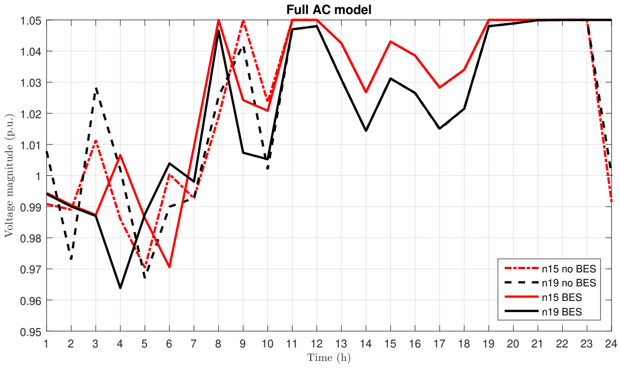

Fig. 6. Voltage magnitudes at buses 15 and 19 with and without the BES for wind penetration level equal to 1

requires more time due to additional binary variables that impose simultaneous charging and discharging. Execution time of the full AC model without the BES is 57.8 s and the number of variables is 8,789. This high number of variables is a result of additional constraints that calculate network losses across transmission lines and voltage levels. Introducing the BES units in the full AC model yields a mixed-integer nonlinear problem (MINLP) and execution time for DICOPT solver is much higher (252 s), while the number of variables is increased to 9,555.

V. Conclusion

This paper proposes and analyzes a formulation for the unit commitment problem considering battery energy storage under the full AC model. We compare its performance with and without the BES and for different factors of wind power penetration levels: 0, 0.5, 1, 1.5. The results show the following main conclusions:

1) By increasing the wind penetration level, TOC of the full AC model is decreased in comparison when there is no wind in the power system: from 61.47% under wind penetration factor 0.5, 93.25% under initial wind penetration factor, and 98.06% under wind penetration factor 1.5.
2) By introducing BES units into the power system, total wind curtailment is generally decreased. The voltage magnitudes are less variable and less dependent on the wind generation since energy storage evens out the copious and scarce wind generation. Also, the number of committed generators is decreased.
3) The full AC formulation requires lower execution time without BES units than the full AC formulation with BES units due to addition of binary variables in the model.

TABLE III
Execution times and number of variables in the models

Model	Without BES		With BES	
	Time (s)	Number of continuous and binary variables	Time (s)	Number of continuous and binary variables
Full AC	57.80	8,789	252.00	9,555

Finally, the formulated AC models contribute with more realistic solutions and provide better insight in the operation of a power system since they capture losses, voltage magnitudes and reactive power flows.

Appendix (Nomenclature)

Sets and Indices

$i \in \Omega^I$ Index of thermal generator i, belonging to set of thermal generators Ω^I.
$l \in \Omega^L$ Index of transmission line l, belonging to set of transmission linesΩ^L.
$n \in \Omega^N$ Index of bus n, belonging to set of network busesΩ^N.
$s \in \Omega^S$ Index of BES unit s, belonging to set of BES units Ω^S.
$t \in \Omega^T$ Index of time period t, belonging to set of periods Ω^T.
$w \in \Omega^W$ Index of wind farm w, belonging to set of wind farms Ω^W.

Parameters:

b_l Series susceptance of transmission line l (S).
$ch_s^{\max}$ Maximum charging power of BES unit s (MW).
$dis_s^{\max}$ Maximum discharging power of BES unit s (MW).
o_i Generating cost of thermal generator i (€/MWh).
$PD_{t,n}$ Active power demand at bus n in period t (MW).
$Pg_i^{\max}$ Maximum active power output of thermal generator i (MW).
$Pw_{t,w}^{\det}$ Maximum power output of wind farm w under wind factor f (MW).
$Pw_{t,w}^{\det,\mathrm{ini}}$ Maximum power output of wind farm w under the initial factor 1 (MW).
$QD_{t,n}$ Reactive power demand at bus n in period t (MVAr).
$Qg_{t,i}^{\max}$ Maximum reactive power output of thermal generator i (MVAr).
$Qg_{t,i}^{\min}$ Minimum reactive power output of thermal generator i (MVAr).
RD_i Maximum ramp down of thermal generator i (MW/h).
RU_i Maximum ramp up of thermal generator i (MW/h).
$S_l^{\max}$ Maximum power rating of transmission line l (MVA).
$soc_{t,s}^{\mathrm{in}}$ Initial value of state of charge of BES unit s (MWh).
$soc_s^{\max}$ Maximum state of charge of BES unit s (MWh).
$V_n^{\max}$ Maximum voltage magnitude at bus n (p.u.).
$V_n^{\min}$ Minimum voltage magnitude at bus n (p.u.).
Y_l Admittance of transmission line l (S).
Z Nominal value that converts from p.u.
ϑ_l Admittance angle of transmission line l (rad).
θ^{max} Maximum allowed voltage angle (rad).
η_s^{ch} Efficiency of charging BES unit s (-).
η_s^{dis} Efficiency of discharging BES unit s (-).

Variables:

$P_{t,l}$ Active power through transmission line l in period t (MW).

$p^{\text{ch}}_{t,s}$ Charging power of BES unit s in period t (MW).

$p^{\text{dis}}_{t,s}$ Discharging power of BES unit s in period t (MW).

$Pg_{t,i}$ Active power output of thermal generator i in period t (MW).

$Pw_{t,w}$ Power output of wind farm w in period t (MW).

$Q_{t,l}$ Reactive power through transmission line l in period t (MVAr).

$Qg_{t,i}$ Reactive power output of thermal generator i in period t (MVAr).

$soc_{t,s}$ State of charge of BES unit s in period t (MWh).

$V_{t,n}$ Voltage magnitude at bus n in period t (rad).

$ws_{t,w}$ Wind spillage of wind farm w in period t (MWh).

$\kappa^{Q\max}_{t,i}$ Slack variable ensuring feasibility of constraint on maximum reactive power output of thermal generator i in period t (MVAr).

$\kappa^{Q\min}_{t,i}$ Slack variable ensuring feasibility of constraint on minimum reactive power output of thermal generator i in period t (MVAr).

$\kappa^{V\max}_{t,n}$ Slack variable helping in ensuring feasibility of constraint on maximum voltage magnitude at bus n in period t (rad).

$\kappa^{V\min}_{t,n}$ Slack variable ensuring feasibility of constraint on minimum voltage magnitude at bus n in period t (rad).

$\theta_{t,n}$ Voltage angle at bus n in period t (rad).

Binary variable:

$x^{\text{ch}}_{t,s}$ Binary variable equal to 1 when BES unit s is being charged during time period t, and 0 otherwise.

REFERENCES

[1] R. Baldick, "The generalized unit commitment problem," *IEEE Transactions on Power Systems*, vol. 10, no. 1, pp. 465-475, 1995.

[2] E. Denny, and M. O'Malley, " Wind generation, power system operation, and emissions reduction," *IEEE Transactions on power systems*, vol. 21, no. 1, pp. 341-347, 2006.

[3] Y. Zhang, V. Gevorgian, C. Wang, X. Lei, E. Chou, R. Yang and L. Jiang, "Grid-Level Application of Electrical Energy Storage: Example Use Cases in the United States and China," *IEEE Power and Energy Magazine*, vol. 15, no. 5, pp. 51-58, 2017.

[4] K. Pandžić, H. Pandžić, I. Kuzle, "Coordination of Regulated and Merchant Energy Storage Investments," *IEEE Transactions on Sustainable Energy*, early access.

[5] H. Pandžić, Y. Wang, T. Qiu, Y. Dvorkin D. S. and Kirschen, "Near-optimal method for siting and sizing of distributed storage in a transmission network," *IEEE Transactions on Power Systems*, vol. 30, no. 5, 2288-2300, 2015.

[6] M. Carrión, Y. Dvorkin and H. Pandžić, "Primary Frequency Response in Capacity Expansion," *IEEE Transactions on Power Systems*, vol. 33, no. 2, pp 1824-1835, 2018.

[7] A. G. Expósito, A. Gomez-Exposito, A. J. Conejo and C. Canizares, "Electric energy systems: analysis and operation," *CRC Press*, 2016.

[8] H. Pandžić, Y. Dvorkin, T. Qiu, Y. Wang and D. S. Kirschen, "Toward cost-efficient and reliable unit commitment under uncertainty," *IEEE Transactions on Power Systems*, vol. 31, no. 2, pp. 970-982, 2016.

[9] Z. Luburić, H. Pandžić and T. Plavšić, "Assessment of Energy Storage Operation in Vertically Integrated Utility and Electricity Market," *Energies*, vol. 10, no. 5, pp. 683, 2017.

[10] K. Bruninx and E. Delarue, "Improved energy storage system and unit commitment scheduling," *in Proceedings of IEEE PowerTech 2017 Manchester*, pp. 1-6, June 2017.

[11] A. Tuohy, P. Meibom, E. Denny and M. O'Malley, "Unit commitment for systems with significant wind penetration," *IEEE Transactions on Power Systems*, vol. 24, no. 2, pp. 592-601, 2009.

[12] A. Papavasiliou, S. S. Oren and B. Rountree, "Applying high performance computing to transmission-constrained stochastic unit commitment for renewable energy integration," *IEEE Transactions on Power Systems*, vol. 30, no. 3, pp. 1109-1120, 2015.

[13] A. Nikoobakht, M. Mardaneh, J. Aghaei, V. Guerrero-Mestre and J. Contreras, "Flexible power system operation accommodating uncertain wind power generation using transmission topology control: an improved linearised AC SCUC model," *IET Generation, Transmission and Distribution*, vol. 11, no. 1, pp. 142-153, 2017.

[14] A. Nasri, S. J. Kazempour, A. J. Conejo and M. Ghandhari, "Network-constrained AC unit commitment under uncertainty: A benders' decomposition approach," *IEEE Transactions on Power Systems*, vol. 31, no. 1, pp. 412-422, 2016.

[15] A. Lotfjou, M. Shahidehpour, Y. Fu and Z. Li, "Security-constrained unit commitment with AC/DC transmission systems," *IEEE Transactions on Power Systems*, vol. 25, no.1, pp. 531-542, 2010.

[16] Y. Fu, M. Shahidehpour and Z. Li, "AC contingency dispatch based on security-constrained unit commitment," *IEEE Transactions on Power Systems*, vol. 21, no. 2, pp. 897-908, 2006.

[17] A. Castillo, C. Laird, C. A. Silva-Monroy, J. P. Watson and R. P. O'Neill, "The unit commitment problem with AC optimal power flow constraints," *IEEE Transactions on Power Systems*, vol. 31, no. 6, pp. 4853-4866, 2016.

[18] C. Grigg, P. Wong, P. Albrecht, R. Allan, M. Bhavaraju, R. Billinton and W. Li, "The IEEE reliability test system-1996. A report prepared by the reliability test system task force of the application of probability methods subcommittee," *IEEE Transactions on Power Systems*, vol. 14, no. 3, pp. 1010-1020, 1996.

[19] H. Pandžić, Y. Dvorkin, T. Qiu, Y. Wang, and D. Kirschen, "Unit Commitment under Uncertainty - GAMS Models," Library of the Renewable Energy Analysis Lab (REAL), University of Washington, Seattle, USA. [Online]. Available at: www.ee.washington.edu/research/real/gams_code.html.